ELSEVIER

Ceramics International 30 (2004) 843–852

CERAMICS INTERNATIONAL

www.elsevier.com/locate/ceramint

Electrophoretic deposition of alumina and zirconia I. Single-component systems

Karel Maca*, Hynek Hadraba, Jaroslav Cihlar

Department of Ceramics, Brno University of Technology, 616 69 Brno, Czech Republic

Received 30 May 2003; received in revised form 17 August 2003; accepted 25 September 2003

Available online 20 March 2004

Abstract

Electrophoretic deposition of Al_2O_3 and ZrO_2 suspended in isopropanol in the presence of monochloroacetic acid and polyvinylbutyral under constant-current conditions was studied. The deposition of ceramic particles occurred on the anode. An optimum deposition in terms of surface flatness, deposit density and thickness was found for 15 wt.% of monochloroacetic acid in isopropanol. The electrophoretic mobility of alumina particles in this suspension was determined from deposition kinetics. The sintering behaviour, hardness, fracture toughness and bending strength of Al_2O_3 and ZrO_2 electrophoretic deposits were comparable with the values measured for the specimens prepared from identical powders by injection moulding and cold isostatic pressing or with the values given in the literature.

Keywords: B. Composites; D. Al_2O_3; D. ZrO_2; Electrophoretic deposition

1. Introduction

Electrophoretic deposition is an experimentally undemanding and comparatively cheap technique enabling the formation of deposits from particles of nanometric dimensions [1,2] to particles of several micrometers in size [3]. Electrophoretic deposition can yield layers of a wide range of thickness, from several nanometers [4] to several millimetres [5,6].

Usually, electrophoretic deposition of Al_2O_3 and ZrO_2 in aqueous medium is described in the literature [7,8]. The advantage of using aqueous suspensions for electrophoretic deposition lies in the easy preparation of stable suspensions of ceramic particles and the ease of controlling the charge on particle surface by changing the pH value of aqueous medium [9]. However, using aqueous solutions results in the electrolysis of water, with gaseous hydrogen generated on the cathode and oxygen on the anode. These gases form bubbles in the deposit, reduce its density and prevent the deposit from adhering to the electrode [7]. On the other side the disadvantage of using suspensions with organic solvents is that the particles are more difficult to stabilize; at the same time suspension stability is the limiting factor with respect to obtaining a deposit of high density [10].

Zhitomirski [11] described electrophoretic deposition of Al_2O_3 and ZrO_2 powders in propanol without admixtures, and at voltages from 50 to 200 V, he deposited within 10–300 s a deposit of 1–10 μm in thickness. By contrast, Harbach and Nienburg [5,6] described a ZrO_2 suspension in pure isopropanol and ethanol as unstable. The authors obtained better results using ZrO_2 dispersed in ethanol and isopropanol stabilized with 4-hydroxybenzoic acid, polyethylenimine and acrylate-acrylamid copolymer. The same authors deposited Al_2O_3 tubes stabilized with trioxydecanoic acid in isopropanol. Will et al. [12] stabilized ZrO_2 powder for deposition in ethanol using polyethylenimine. Ishihara and coworkers [13,14] tested a great number of solvents from the viewpoint of the surface quality of the ZrO_2 deposit. They obtained the best results when using acetylacetone, in which he stabilized the ZrO_2 particles by means of iodine. Chen and Liu [15] used iodine to stabilize ZrO_2 particles in a mixture of one volume part of ethanol (which improved the resistance of the deposit to cracking during drying) and three volume parts of acetone (which improved the surface quality of the deposit). Basu et al. [16] deposited dried ZrO_2 from anhydrous medium of glacial acetic acid.

Most of the references describe electrophoretic deposition at a constant voltage [5,8,9,11,15,17–19]. In this

* Corresponding author. Fax: +420-541143202.
E-mail address: maca@umi.fme.vutbr.cz (K. Maca).

0272-8842/$30.00
doi:10.1016/j.ceramint.2003.09.021

case, however, the weight increment of the deposit with time declines rapidly or even stops completely because the density of electric current decreases due to increasing resistance of the system. This problem does not appear in the constant-current mode [6,20].

It has been established recently that in isopropanol suspensions stabilized with monochloroacetic acid the Al_2O_3 and ZrO_2 particles have a negative charge [21]. Electrophoretic deposition, which in such cases occurs on the anode, has not so far been described for these systems in the literature. The aim of the present work was therefore to prepare Al_2O_3 and ZrO_2 deposits from isopropanol suspensions stabilized with monochloroacetic acid. Attention was mainly focused on optimizing the suspension composition and describing the sintering kinetics, resultant microstructure and mechanical properties of these deposits.

2. Experimental

2.1. Materials

The Al_2O_3 and ZrO_2 ceramic powder materials used for electrophoretic deposition are summarized in Table 1. Isopropanol (p.a., Onex, Czech Republic) was used as the dispersion medium for the preparation of the suspensions of Al_2O_3 and ZrO_2 powders. Monochloroacetic acid (MCAA; p.a., Lachema, Czech Republic) was used as the stabilizing and dispersing aid and polyvinylbutyral (PVB; Butvar B79, Monsanto, USA) was used as a binder. The water content in the suspensions was reduced to minimum by drying the ceramic powders at 130 °C/2 h while isopropanol was dried over calcium for several hours and subsequently distilled until its water content was less than 0.01% (as shown by gas chromatography analysis).

2.2. Suspension composition

The suspensions were prepared by mixing 15 wt.% of Al_2O_3 or ZrO_2 powder in 85 wt.% of the liquid phase that was prepared by dissolving 1, 2, 5, 15 or 25 wt.% of MCAA and (in the case of Al_2O_3 suspension) 0, 1, 2 or 4 wt.% of PVB in isopropanol. A complete factor experiment for optimizing suspension composition with all MCAA and PVB concentration levels was conducted with type HP Al_2O_3. All MCAA concentration levels were also used with type 3YS ZrO_2. The study of suspension sedimentation, sintering kinetics and mechanical properties of deposits was carried out on only one selected concentration level of MCAA and PVB. The exact composition of all the suspensions used is given in Table 2.

2.3. Electrophoretic deposition

A schematic section through a horizontal electrophoretic cell is given in Fig. 1. The electrodes made of stainless steel with polished surface were at a constant distance of 26 mm, their effective areas were in the shape of a trapezoid of 15 cm^2. The volume of suspension in the electrophoretic cell was 80 ml. A stabilized source controlled by microcomputer (E815, Consort, Belgium) was used as the voltage and current source. All experiments were conducted in the 5 mA constant-current mode.

The depositions employed to optimize the suspension composition (Section 3.1) were performed by continuous electrophoretic deposition lasting 30 min.

When studying the effect of suspension sedimentation on the course of deposition (Section 3.2), interrupted depositions taking a total of 60–80 min were performed. With every interruption of the deposition the deposit thickness was measured, namely at 18, 38 and 58 mm below the suspension level and subsequently the suspension was or was not stirred. In the case of deposition without stirring the drop in the suspension top level (which contrasted with the volume of clear solvent without ceramic powder—the supernatant) was read during the deposition time. These readings were used to establish the mean velocity of sedimentation (v_s). The resultant shape of the deposit was determined by measuring its thickness at 22 equidistant vertical depths.

Deposits of a larger thickness, designed for the study of sintering (Section 3.3) and mechanical properties (Section 3.4), were obtained by interrupted deposition, i.e. a sequence of consecutive depositions from one suspension, with the suspension stirred between every two depositions. Every partial deposition lasted 5 min, the total deposition time was 120–160 min.

Table 1
Ceramic powder materials used for electrophoretic deposition

Marking	Material	Manufacturer	Manufacturer's marking	Mean particle size (μm)[a]	Mean agglomerate size (μm)[b]
HP	Al_2O_3[c]	Malakoff Ind. (USA)	RC HP DBM	0.47	0.6
UFX	Al_2O_3[c]	Malakoff Ind. (USA)	RC UFX DBM	0.33	0.4
3Y	ZrO_2[d]	Tosoh (Japan)	TZ-3Y	0.25	0.7
3YS	ZrO_2[d]	Tosoh (Japan)	TZ-3YS	0.12	0.7

[a] Established from microphotographs.
[b] Established by laser diffraction (Horiba LA-500, Japan).
[c] With an addition of 0.05 wt.% MgO.
[d] Stabilized by 3 mol.% Y_2O_3.

Table 2
Composition of suspensions

Suspension	Al_2O_3 (wt.%)	ZrO_2 (wt.%)	Isopropanol (wt.%)	MCAA (wt.%)	PVB (wt.%)	Used in section(s)
HP-1-0	15	0	84.15	0.85	0	3.1
HP-2-0	15	0	83.30	1.70	0	3.1
HP-5-0	15	0	80.75	4.25	0	3.1
HP-15-0	15	0	72.25	12.75	0	3.1, 3.2, 3.3, 3.4
HP-25-0	15	0	63.75	21.25	0	3.1
HP-1-1	15	0	83.16	0.84	1	3.1
HP-2-1	15	0	82.32	1.68	1	3.1
HP-5-1	15	0	79.80	4.20	1	3.1
HP-15-1	15	0	71.40	12.60	1	3.1
HP-25-1	15	0	63.00	21.00	1	3.1
HP-1-2	15	0	82.17	0.83	2	3.1
HP-2-2	15	0	81.34	1.66	2	3.1
HP-5-2	15	0	78.85	4.15	2	3.1
HP-15-2	15	0	70.56	12.45	2	3.1
HP-25-2	15	0	62.25	20.75	2	3.1
HP-1-4	15	0	80.20	0.81	4	3.1
HP-2-4	15	0	79.38	1.62	4	3.1
HP-5-4	15	0	76.95	4.05	4	3.1
HP-15-4	15	0	68.85	12.15	4	3.1
HP-25-4	15	0	60.75	20.25	4	3.1
3YS-1-0	0	15	84.15	0.85	0	3.1
3YS-2-0	0	15	83.30	1.70	0	3.1
3YS-5-0	0	15	80.75	4.25	0	3.1
3YS-15-0	0	15	72.25	12.75	0	3.1, 3.3, 3.4
3YS-25-0	0	15	63.75	21.25	0	3.1
UFX-15-0	15	0	72.25	12.75	0	3.3, 3.4
3Y-15-0	0	15	72.25	12.75	0	3.3, 3.4

2.4. Evaluation of deposit properties

All the deposits together with the electrodes were first dried at room temperature for 24 h and at 70 °C for 1 h, after which they were removed from the electrodes, annealed (800 °C/1 h) and sintered (1500 °C/2 h) in air atmosphere.

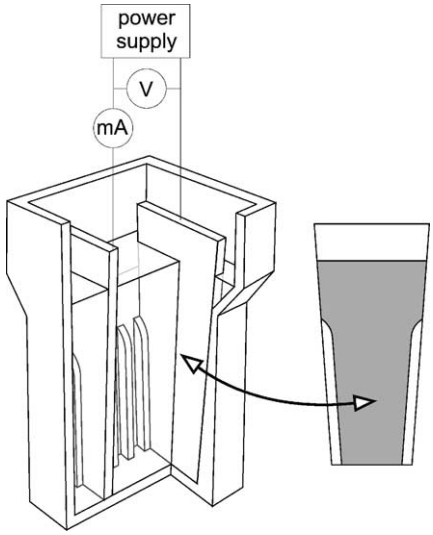

Fig. 1. Section through the cell used for electrophoretic deposition of ceramic materials.

The quality of the deposit surface subsequent to drying was evaluated visually. The relative density of the annealed deposit (ρ_{800}) was established from soaking capacity and the relative density of the sintered deposit (ρ_{1500}) was established by the Archimedes method (EN 623-2). The pore size distribution was established by mercury porosimetry (Carlo Erba 200, Italy).

The sintering process was monitored by a high-temperature dilatometer (L75/50, Linseis, Germany). The relative length change in the deposit as a function of time and temperature was measured in two directions, namely in the direction of particle motion during electrophoretic deposition (longitudinal direction—marked by index "*L*") and in perpendicular direction to the particle motion during the deposition (transversal direction—marked by index "*T*"). The dimensionless coefficient of specimen shrinkage anisotropy (k) was calculated according to the relation:

$$k = \frac{\varepsilon_T}{\varepsilon_L} \quad (1)$$

where ε_L is the final deposit relative shrinkage in the longitudinal direction, and ε_T is the final deposit relative shrinkage in the transversal direction. The coefficient of thermal expansion (CTE) was calculated from the cooling curves of

sintered deposits. The temperature dependence of relative specimen density ($\rho_{rel}(T)$) was calculated from the values of final densities and from the shrinkage curve $\varepsilon(T)$ (first, the specimen elongation due to simple thermal expansion of the material was subtracted from the elongation values measured).

Polished specimens of sintered deposits were thermally etched and made conductive by applying three layers of gold coating and then studied by SEM (Philips XL30, the Netherlands). The grain size of sintered ceramics (d_G) was determined by computer image analysis (Atlas Software, Tescan, Czech Republic) from microphotographs of etched deposit sections. The value of equivalent diameter, calculated from the area of grains, was used as the mean grain size (d_G).

The indentation fracture toughness of sintered deposits was measured by the indentation method (according to Japanese Industrial Standard JIS R 1607). The Vickers hardness tester was used as the indentor. The fracture toughness (K_{IC}) of materials was calculated using the values of the length of indentation crack (c), indentation force ($F = 98$ N), Young's modulus of ZrO_2 ($E_Y = 380$ GPa [19]) and Al_2O_3 ($E_Y = 210$ GPa [19]) and hardness (HV) according to the relation given in JIS R 1607. The hardness of material was determined from the size of the diagonal of the hardness tester tip indentation in the surface of material caused by indentation force F.

The four-point flexure strength (EN 843-1) was only measured for Al_2O_3 deposits (type HP). The test specimens were cut with a diamond disk from deposits annealed at 1000 °C/1 h. The test specimens were then sintered at 1500 °C/2 h. The sintered specimens were ground to be 2 mm × 2.5 mm × 25 mm and the tensile side was polished with diamond paste of 1 μm grain size. Bending strength was measured on a universal test machine (Z020, Zwick, Germany) with a jig for bending strength measurement.

3. Results and discussion

3.1. Optimization of suspension composition

The suspensions with type HP Al_2O_3 and type 3YS ZrO_2 were used for the optimization experiments (see Table 2). The Al_2O_3 and ZrO_2 particles were charged negatively and the layer was deposited on the anode, in the same way as in work of Cihlar et al. [21].

The smoothness of deposit surface, deposit thickness and density were affected by suspension composition (the contents of monochloroacetic acid and polyvinylbutyral). The deposit had a smooth surface if the deposition was from a suspension containing more than 4 wt.% of monochloroacetic acid, irrespective of the PVB concentration. This phenomenon was probably due to the effect of MCAA concentration on electrophoretic behaviour of the suspension. The intensity of electric field during deposition was dependent on the contents of monochloroacetic acid and

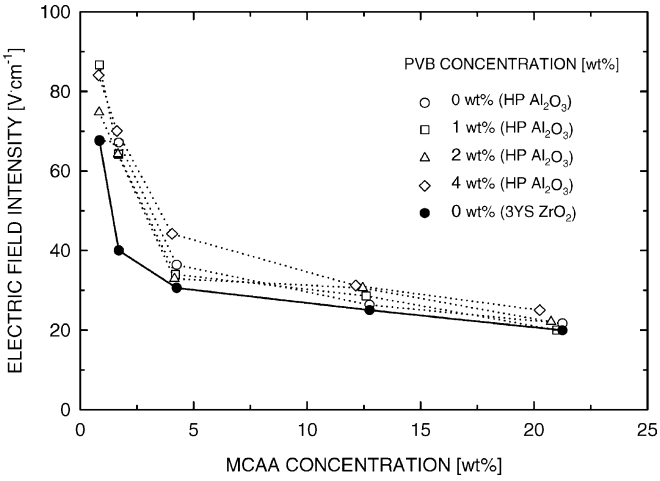

Fig. 2. Dependence of electric field intensity during deposition of alumina and zirconia on the concentration of MCAA and PVB in the suspension.

polyvinylbutyral in the suspension (see Fig. 2). The drop in the intensity of electric field with increasing concentration of monochloroacetic acid was probably due to the increasing conductivity of the solution, which in the case of Al_2O_3 suspensions increased from 2.9×10^{-4} S m^{-1} (HP-1-0) [21] to 23.8×10^{-4} S m^{-1} (HP-25-0) [21]. The relation between velocity of particle motion (v), electrophoretic mobility (μ) and electric field intensity (E) is given by the equation:

$$v = \mu \times E. \quad (2)$$

Since electrophoretic mobility of the Al_2O_3 and ZrO_2 particles at an MCAA concentration of more than 0.85 wt.% is independent of its concentration [21], the velocity of the particles in the suspension decreased with decreasing electric field intensity and thus with increasing MCAA concentration. The slower motion of particles probably led to their more effective arrangement on the anode, which was confirmed by the higher green density of deposits with a higher MCAA content (see Fig. 3). The final relative deposit

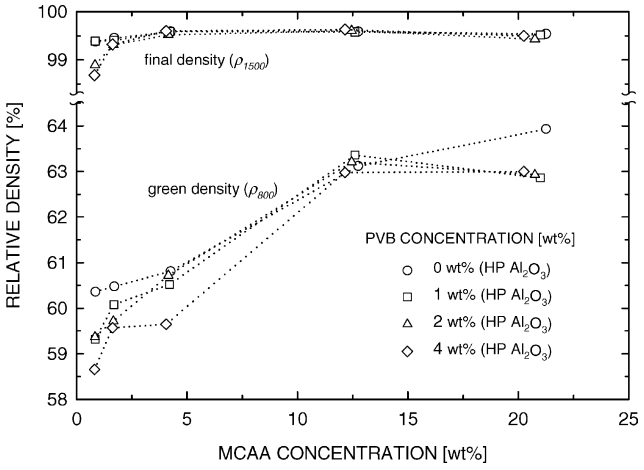

Fig. 3. Dependence of the relative density of alumina deposit after annealing and sintering on the concentration of MCAA and PVB in the suspension.

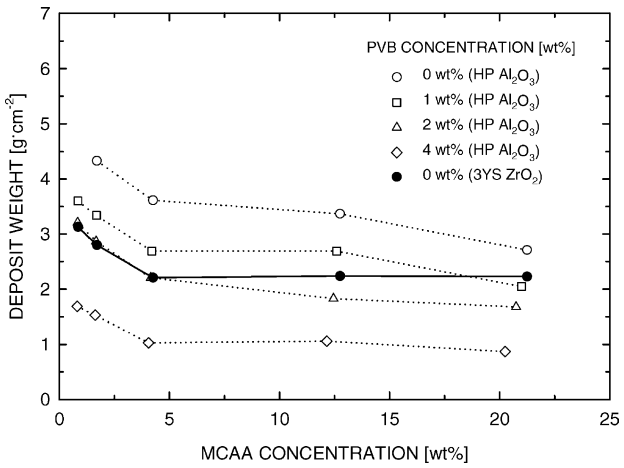

Fig. 4. Dependence of alumina and zirconia deposit weight on the concentration of MCAA and PVB in the suspension.

density was ca. 99.5% and was independent of both PVB and MCAA concentration (provided MCAA concentration exceeded 4 wt.%).

As can be seen from Fig. 2, the addition of polyvinylbutyral to the suspension led to a slight increase in electric current intensity during deposition. As established in work of Cihlar et al. [21], increasing polyvinylbutyral content reduced the electrophoretic mobility of particles, which led to a lower weight of the deposit. This result has also been proved in the present work as can be seen from Fig. 4, which illustrates the dependence of deposit weight on MCAA and PVB concentrations. The electrophoretic mobility of particles is given by the Henry equation [22]:

$$\mu = \frac{2}{3}\frac{\varepsilon\zeta}{\eta} f(R\kappa^{-1}) \tag{3}$$

where ε is the permittivity of the medium, ζ is the zeta potential, η is the dynamic viscosity of the medium, and $f(Rk^{-1})$ is the function of the product of particle radius (R) and the thickness of electric double layer (k^{-1}). The drop in the electrophoretic mobility of particles in the suspension was due to the reduction in the ζ-potential of particles and the increase in the viscosity of the medium caused by the content of polyvinylbutyral in the suspension [21].

The addition of polyvinylbutyral had no positive effect on either the final deposit density (see Fig. 3) or the flatness of their surfaces. Since it reduced the electrophoretic mobility of particles in the suspension, it had a negative effect on deposit weight (Fig. 4).

From the viewpoint of the flatness of deposit surface, which is important, for example, in the deposition of layered composites [23], the optimum amounts were 15 and 25 wt.% of MCAA in isopropanol. At a concentration of 15 wt.% of MCAA, the deposit yield was, of course, higher (see Fig. 4). On the basis of the above results the suspensions containing no PVB and with a 15 wt.% content of MCAA in the liquid phase (i.e. 12.75 wt.% in the suspension) were evaluated as optimum suspensions.

3.2. Suspension sedimentation and its elimination

The deposits obtained in the previous part of the work were of non-constant thickness, which increased continuously towards the bottom of electrophoretic cell. The reason lay in suspension sedimentation due to earth's gravitation, which in the case of horizontal arrangement of the electrophoretic cell is perpendicular to the direction of electrophoretic force. The following experiments, which were conducted with the HP-15-0 suspension on the basis of the results of the preceding section, had as their aim the description and elimination of suspension sedimentation and its consequences.

The first to be studied was deposition with the interrupted deposition mode, during which the deposit thickness was measured continuously but the suspension was not stirred. The dependence of deposit thickness on time at three depths below the suspension level is given in the graph of Fig. 5. It can be seen from the graph that after some time the deposit thickness values differed with the place of measurement because sedimentation occurred in the suspension.

To prevent the sedimentation of powder, the suspension had to be stirred. Since after 5 min of deposition without stirring no differences in deposit thickness could be observed at the individual levels of measuring (see Fig. 5), the 5-min interval was chosen as appropriate for stirring the suspension. Fig. 6 gives the dependence of deposit thickness on time as obtained for interrupted deposition with suspension stirring. It can be seen that the deposition was uniform at all the three levels observed. In the case that particle concentration in the suspension in vertical direction does not change (the suspension does not sediment or it is stirred) the dependence of deposit weight (m) on time (t) is given by the Zhang equation [24] (m_0 is the initial weight of powder in suspension and d is the distance between electrodes):

$$m = m_0(1 - \mathrm{e}^{-(\mu E/d)t}) \tag{4}$$

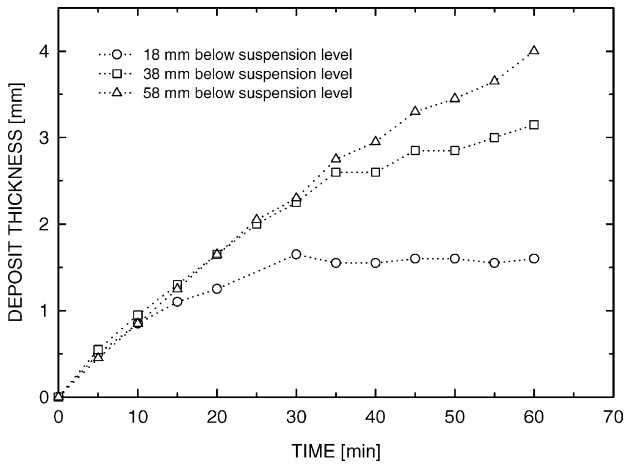

Fig. 5. Dependence of alumina (type HP) deposit thickness on deposition time and on the vertical position (non-stirred suspension).

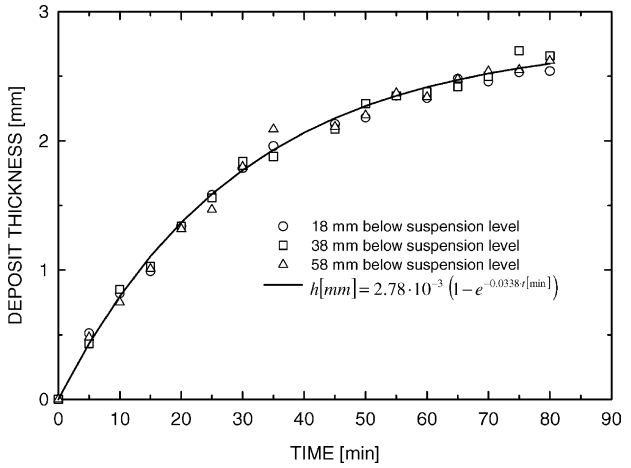

Fig. 6. Dependence of alumina (type HP) deposit thickness on deposition time and on the vertical position (the suspension was stirred at intervals of 5 min).

Across the whole of its area a deposit from such a suspension should have a constant thickness h, which can be calculated from the relation:

$$h = \frac{100\, m_0}{S \rho_{\text{theor}} \rho_{\text{rel}}} (1 - \mathrm{e}^{-(\mu E/d)t}) \quad (5)$$

where S is the electrode surface, ρ_{theor} is the theoretical ceramics density and ρ_{rel} is the relative deposit density after deposition.

As can be seen, the experimental data in Fig. 6 can be fitted well with the curve:

$$h\ (\text{mm}) = 2.78(1 - \mathrm{e}^{-0.0338 \cdot t\ (\text{min})}) \quad (6)$$

Comparing Eq. (6) with Eq. (5) (with $S = 15\,\text{cm}^2$, $d = 26\,\text{mm}$, $E = 30.8\,\text{V cm}^{-1}$, $\rho_{\text{rel}} = 60\%$), the values $m_0 = 10.0\,\text{g}$ and $\mu = 0.475\,\mu\text{m cm V}^{-1}\,\text{s}^{-1}$ were calculated. The actual amount of particles in the suspension was 11.6 g, which was in good agreement with the calculated value 10.0 g. The difference may have been due to partial sedimentation of the powder, estimation of the relative deposit density from the density value of the dried specimen or the electrophoretic cell geometry, when part of the suspension was behind the electrodes (see Fig. 1). The calculated mobility value was in good agreement with the mobility $\mu = 0.275\,\mu\text{m cm V}^{-1}\,\text{s}^{-1}$ as established on a Zetasizer apparatus for a similar but 100× diluted suspension in ac electric field [21].

Now that we know the electrophoretic mobility of particles in the suspension, we can venture a theoretical description of the shape of deposit cross section in dependence on time and on the depth below suspension level even for the case of non-stirred, that is to say sedimenting suspension, according to the relation:

$$h\ (\text{mm}) = 2.78(1 - \mathrm{e}^{-0.0338(H - x/v_{\text{S}})}) \quad (7)$$

where H (mm) is the initial height of suspension level (65 mm), x (mm) is the vertical distance from the bottom

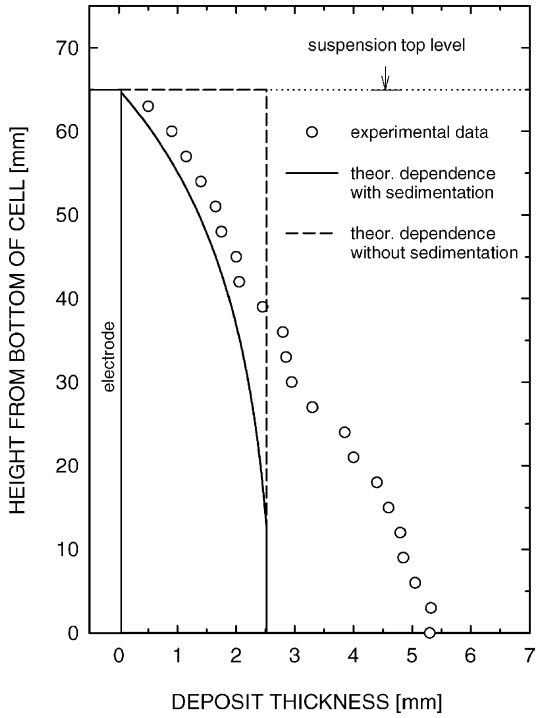

Fig. 7. Dependence of alumina (type HP) deposit thickness on the height from the bottom of electrophoretic cell.

of electrophoretic cell and v_{S} is the sedimentation velocity established as described in the experimental part and found to be $0.75\,\text{mm min}^{-1}$. Fig. 7 gives a comparison of the theoretical calculated deposit shape with the experimentally established shape subsequent to a 70-min deposition of Al_2O_3 (type HP) without stirring the suspension. As can be seen, in the upper part of the electrode the deposit shape corresponded with the theoretical dependence but in the lower part the deposit thickness was larger than it would be on the assumption that the ceramic powder settles on the bottom. It seems that the powder did not settle on the bottom but whirled in the lower part of the cell and at the same time deposited on the electrode.

3.3. Sintering kinetics and the resultant microstructure of Al_2O_3 and ZrO_2 deposits

For the preparation of all the types of materials studied below, interrupted electrophoretic deposition was used, coupled with suspension stirring at interrupted deposition every 5 min. The suspension contained 15 wt.% of the ceramic phase and 12.75 wt.% of MCAA (see Table 2). The properties of the deposits established during sintering and by evaluating their microstructure are summarized in Table 3.

The relative deposit density after annealing decreased with decreasing particle size. The relative density of Al_2O_3 and ZrO_2 deposits after sintering was higher than 99%, with the exception of type UFX Al_2O_3 deposit, whose final relative density was ca. 98.6%. The ZrO_2 material reached almost the theoretical density although it exhibited very low green

Table 3
Selected properties of ceramic deposits after annealing and sintering

Material type	ρ_{800} (%)	s/n (%/−)[a]	ρ_{1500} (%)	s/n (%/−)[a]	$k = \varepsilon_T/\varepsilon_L$ (−)	CTE × 10^{-6} (K^{-1})	d_G (μm)
HP-L	62.2	0.3/6	99.2	0.2/3	0.77	8.7	1.93
HP-T			99.2	0.1/3		9.0	
UFX-L	58.5	0.3/6	98.5	0.4/3	0.81	9.3	2.22
UFX-T			98.7	0.1/3		9.1	
3YS-L	47.0	0.2/6	99.6	0.8/3	0.96	9.7	0.55
3YS-T			99.7	0.2/3		10.7	
3Y-L	41.6	0.3/6	99.8	0.2/3	0.98	9.5	0.55
3Y-T			99.9	0.1/3		10.5	

[a] s is standard deviation and n is number of measurements.

density. This is because the sinterability of a green body is not given by the absolute value of its porosity but by the pore size distribution, in particular by the ratio of the radius of the largest pores and the particle size [25,26].

A shrinkage anisotropy was found in Al_2O_3 specimens in the longitudinal direction (L) and in the transversal direction (T). Specimen shrinkage was higher in the direction of particle motion (L). Shrinkage anisotropy was also established for prism-shaped bodies prepared by injection moulding of type HP Al_2O_3 powder [27] and another type of alumina powder [28], with the shrinkage in perpendicular direction to injection direction being higher. This anisotropy was explained by the longer axes of elongated Al_2O_3 particles being arranged in parallel with injection direction [28]. Accepting this hypothesis would mean that in the deposit the particles settle with their longer dimension running parallel with the electrode plane although in the suspension the particles flow with their longer dimension perpendicular to the electrode to minimize the medium's resistance. Similarly, Dalzell and Clark [29] observed a tendency of SiC fibres in Al_2O_3 matrix to be oriented in parallel to the electrode. In the ZrO_2 deposits with spherical particles the shrinkage anisotropy during sintering was negligible.

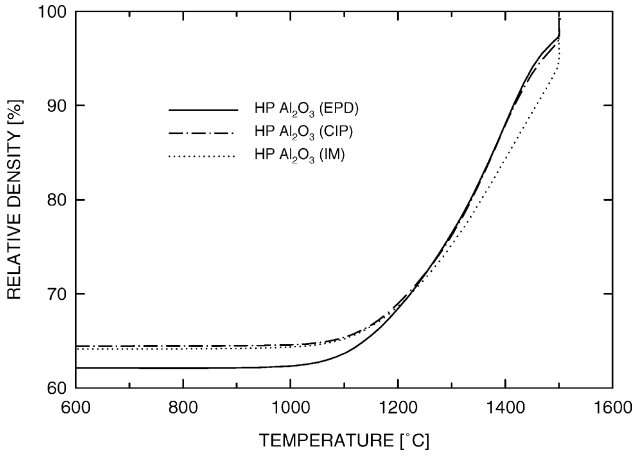

Fig. 8. Sintering kinetics of alumina (type HP) prepared by electrophoretic deposition (EPD), injection moulding (IM) and cold isostatic pressing (CIP).

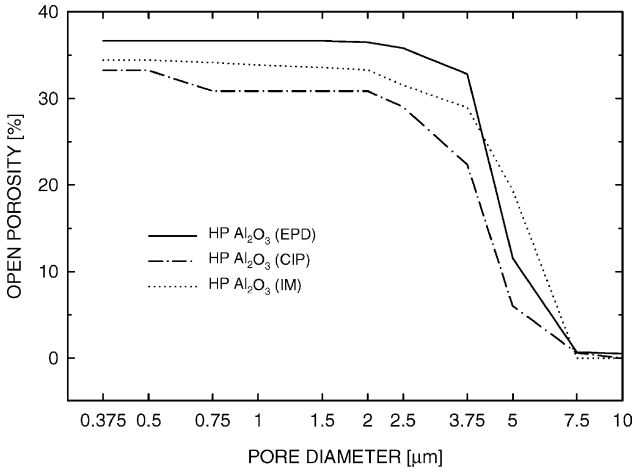

Fig. 9. Pore size distribution of alumina (type HP) prepared by electrophoretic deposition (EPD), injection moulding (IM) and cold isostatic pressing (CIP).

In work of Maca et al. [30], the coefficient of thermal expansion of injection-moulded and isostatically pressed Al_2O_3 of the type of HP was established, CTE (Al_2O_3) = 9 × 10^{-6} K^{-1}, and also of ZrO_2 of the type of 3Y, prepared in the same way, CTE(ZrO_2) = 11 × 10^{-6} K^{-1}. These values are approximated more by the values measured on specimens in the transversal direction. The values of the coefficients of thermal expansion in the longitudinal direction carried a large measuring error since the length of the specimens was too small.

Although the specimen prepared by electrophoretic deposition was of low green density, its sintering kinetics was comparable with that of the specimen prepared by cold isostatic pressing, and better than in the case of the specimen prepared by injection moulding (Fig. 8). This means that the arrangement of particles and pores in the course of electrophoretic deposition was homogeneous, which was also confirmed by mercury porosimetry of green bodies (Fig. 9).

Fig. 10 gives the photographs of the microstructure of Al_2O_3 and ZrO_2 deposits. The mean grain size (d_G) established by image analysis from the microstructure photographs is given in Table 3. The size of Al_2O_3 grains was

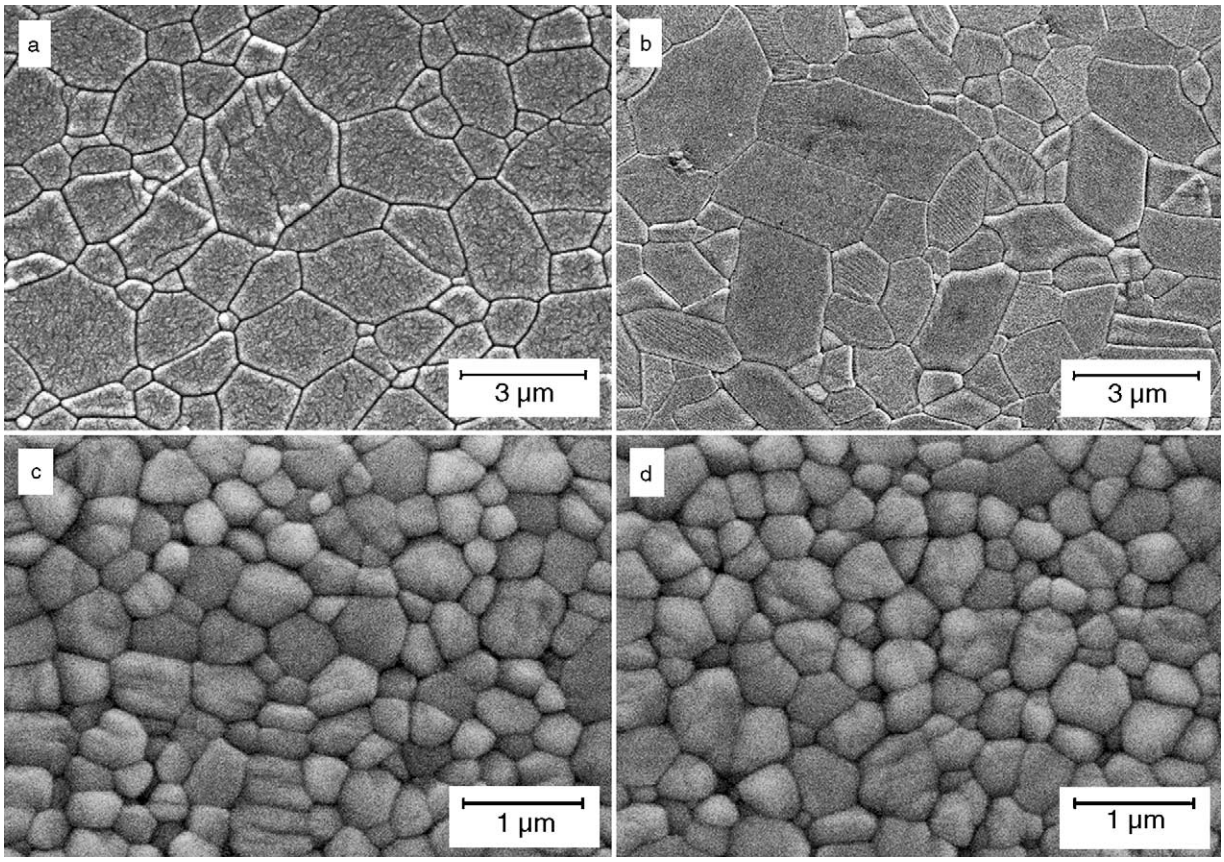

Fig. 10. Microstructure of sintered alumina and zirconia ceramics prepared by intermittent electrophoretic deposition: (a) type HP alumina, (b) type UFX alumina, (c) type 3YS zirconia and (d) type 3Y zirconia.

Table 4
Hardness, indentation crack length and fracture toughness of Al_2O_3 and ZrO_2 deposits

Material type	Hardness		Indentation crack length		Fracture toughness	
	HV (GPa)	s (Pa)/n	l_c (μm)	s (μm)/n	K_{IC} (MPa m$^{0.5}$)	s (MPa m$^{0.5}$)/n
HP	17.8	0.5/20	138	17/20	5.2	1.1/20
UFX	18.0	0.6/20	123	11/20	6.0	0.7/20
3YS	12.9	0.1/20	89	6/20	8.6	0.9/20
3Y	12.9	0/20	82	4/20	9.6	0.7/20

ca. 2 μm while the grain size of type 3YS ZrO_2 and type 3Y ZrO_2 was 0.55 μm. The slight increase in ZrO_2 grains when compared with the initial powder size was not surprising, it was also observed by other authors [31] and it was explained as the effect of its tetragonal structure on the mobility of grain boundaries. For comparison, the grain size of type HP Al_2O_3 prepared by injection moulding and sintering at 1530 °C/2 h was 1.6 μm, that of type 3YS ZrO_2 prepared by injection moulding and sintering at 1500 °C/2 h was 0.4 μm (established by linear intercept method) [32].

3.4. Mechanical properties of Al_2O_3 and ZrO_2 deposits

The hardness, indentation crack length and fracture toughness of Al_2O_3 and ZrO_2 deposits are given in Table 4. The hardness of type HP Al_2O_3 deposit and that of type UFX Al_2O_3 deposit was practically the same, 17.9 and 18.0 GPa, respectively. The hardness of ZrO_2 deposits was also identical: 12.9 GPa for both types of ZrO_2. The hardness values of the deposits are comparable with the values given in the literature: 18 GPa in the case of Al_2O_3 [33] and 12.4 GPa in the case of ZrO_2 [34].

The ZrO_2 deposits exhibited higher fracture toughness than the Al_2O_3 deposits, which is an anticipated result, caused by transformation toughening with yttria-stabilized ZrO_2.

The mean bending strength σ_m of type HP Al_2O_3 prepared by interrupted electrophoretic deposition in four-point flexure was 625 MPa with standard deviation $s = 87$ MPa. The strength values of bodies were described by the Weibull probability distribution, with the corresponding

strength value $\sigma_{m0} = 662$ MPa and the Weibull distribution parameter $m_W = 8.6$. The bending strength of Al_2O_3 prepared by electrophoretic deposition was examined on bodies of 2 mm × 2.5 mm × 20 mm. With the aid of the loaded volume unit [35] the bending strength value found for bodies of 2 mm × 2.5 mm × 20 mm can be converted to the bending strength value corresponding to bodies of 3 mm × 4 mm × 40 mm. After this recalculation the bending strength of alumina prepared by electrophoretic deposition was $\sigma_{m0} = 553$ MPa. This bending strength value was comparable with those of type HP Al_2O_3 prepared by injection moulding (515 MPa) and cold isostatic pressing (464 MPa).

4. Conclusion

Electrophoretic deposition of alumina and zirconia from isopropanol suspension in the presence of monochloroacetic acid using 5 mA constant current occurred on the anode. With increasing content of monochloroacetic acid in the suspension the electric field intensity necessary to generate a constant current of 5 mA decreased, leading to a lower velocity of the particles and a more effective arrangement of these particles on the electrode. With the content of monochloroacetic acid in the suspension exceeding 12.15 wt.%, deposits with flat surface were obtained which sintered at 1500 °C to a density higher than 99% TD. The electrophoretic mobility of alumina particles in this suspension was 0.48 μm cm V^{-1} s^{-1}.

The hardness, bending strength and fracture toughness of electrophoretically deposited Al_2O_3 and ZrO_2 materials were comparable with the values given in the literature and EPD is therefore an effective way to produce low cost components with good properties.

Acknowledgements

This work was supported by the Czech Ministry of Education by the Grant No. VZ CEZ: J22/98.

References

[1] N. Ogata, J. Van Tassel, C.A. Randall, Electrode formation by electrophoretic deposition of nanopowders, Mater. Lett. 49 (2001) 7–14.
[2] L. Biao Lai, D.-H. Chen, T.-C. Huang, Preparation and characterization of Ti-supported nanostructured Pt electrodes by electrophoretic deposition, Mater. Res. Bull. 36 (2001) 1049–1055.
[3] I. Zhitomirski, Cathodic electrophoretic deposition of diamond particles, Mater. Lett. 37 (1998) 72–78.
[4] S.Y. Zhao, S.B. Lei, S.H. Chen, H.Y. Ma, S.Y. Wang, Assembly of two-dimensional ordered monolayers of nanoparticles by electrophoretic deposition, Colloid Polym. Sci. 278 (2000) 682–686.
[5] F. Harbach, H. Nienburg, Homogenous functional ceramic components through electrophoretic deposition from stable colloidal suspensions—I. Basic concepts and application to zirconia, J. Eur. Ceram. Soc. 18 (1998) 675–683.
[6] F. Harbach, H. Nienburg, Homogenous functional ceramic components through electrophoretic deposition from stable colloidal suspensions—II. Beta-alumina and concepts for industrial production, J. Eur. Ceram. Soc. 18 (1998) 685–692.
[7] T. Uchikoshi, K. Ozawa, B.D. Hatton, Y. Sakka, Dense, bubble-free ceramic deposits from aqueous suspensions by electrophoretic deposition, J. Mater. Res. 16 (2001) 321–324.
[8] J.Y. Choudhary, H.S. Ray, K.N. Rai, Electrophoretic deposition of alumina from aqueous suspensions, Trans. J. Br. Ceram. Soc. 81 (1982) 189–193.
[9] R. Clasen, S. Janes, Ch. Oswald, D. Ranker, Electrophoretic deposition of nanosized ceramic powders, Adv. Ceram. 21 (1987) 481–486.
[10] P. Sarkar, P.S. Nicholson, Electrophoretic deposition (EPD): mechanism, kinetics and application to ceramics, J. Am. Ceram. Soc. 79 (1996) 1987–2002.
[11] I. Zhitomirski, Electrophoretic and electrolytic deposition of ceramic coatings on carbon fibers, J. Eur. Ceram. Soc. 18 (1998) 849–856.
[12] J. Will, M. Hruschka, L. Gubler, L.J. Gauckler, Electrophoretic deposition of zirconia on porous anodic substrates, J. Am. Ceram. Soc. 84 (2001) 328–332.
[13] T. Ishihara, K. Sato, Y. Takita, Electrophoretic deposition of Y_2O_3-stabilized ZrO_2 electrolyte films in solid oxide fuel cells, J. Am. Ceram. Soc. 79 (1996) 913–919.
[14] T. Ishihara, K. Shimose, T. Kudo, H. Nishiguchi, T. Akbay, Y. Takita, Preparation of yttria-stabilized zirconia thin films on strontium-doped $LaMnO_3$ cathode substrates via electrophoretic deposition for solid oxide fuel cells, J. Am. Ceram. Soc. 83 (2000) 1921–1927.
[15] F. Chen, M. Liu, Preparation of yttria-stabilized (YSZ) films on $La_{0.85}Sr_{0.15}MnO_3$ (LSM) and LSM-YSZ substrates using an electrophoretic deposition (EPD) method, J. Eur. Ceram. Soc. 21 (2001) 127–134.
[16] R.N. Basu, C.A. Randall, M.J. Mayo, Fabrication of dense zirconia electrolyte film for tubular solid oxide fuel cells by electrophoretic deposition, J. Am. Ceram. Soc. 84 (2001) 33–40.
[17] P. Sarkar, X. Haung, P.S. Nicholson, Structural ceramic microlaminates by electrophoretic deposition, J. Am. Ceram. Soc. 75 (1999) 2907–2909.
[18] O. Prakash, P. Sarkar, P.S. Nicholson, Crack deflection in ceramic/ceramic laminates with strong interfaces, J. Am. Ceram. Soc. 78 (1995) 1125–1127.
[19] B. Hatton, P.S. Nicholson, Design and fracture of layered Al_2O_3/TZ3Y composites produced by electrophoretic deposition, J. Am. Ceram. Soc. 84 (2001) 571–576.
[20] P.S. Nicholson, P. Sarkar, The electrophoretic deposition of ceramics, Adv. Ceram. 21 (1987) 469–479.
[21] J. Cihlar, Z. Cihlarova, H. Hadraba, Influence of weak acids on electrophoretic behavior of alcoholic suspensions of alumina and zirconia, submitted for publication.
[22] P.C. Hiemenz, R. Rajagopalan, Principles of Colloid and Surface Chemistry, Marcel Dekker, New York, 1997.
[23] H. Hadraba, K. Maca, J. Cihlar, Electrophoretic deposition of alumina and zirconia—II. Two-component systems, Ceram. Int. 30 (2004) 853–863.
[24] Z. Zhang, Y. Huang, Z. Jiang, Electrophoretic deposition forming of SiC-TZP composites in a nonaqueous sol media, J. Am. Ceram. Soc. 77 (1994) 1946–1949.
[25] J. Zheng, J.S. Reed, Effects of particle packing characteristics on solid-state sintering, J. Am. Ceram. Soc. 72 (1989) 810–817.
[26] M.N. Rahaman, L.C. De Jonghe, M.-Y. Chu, Effect of green density on densification and creep during sintering, J. Am. Ceram. Soc. 74 (1991) 514–519.
[27] M. Trunec, J. Cihlar, Thermal removal of multicomponent binder from ceramic injection mouldings, J. Eur. Ceram. Soc. 22 (2002) 2231–2241.

[28] S. Krug, J.R.G. Evans, J.H.H. ter Maat, Differential sintering in ceramic injection moulding: particle orientation effect, J. Eur. Ceram. Soc. 22 (2002) 173–181.
[29] W.J. Dalzell, D.E. Clark, Thermophoretic and electrophoretic deposition of sol–gel composite coatings, Ceram. Eng. Sci. Proc. 7 (1986) 1014–1026.
[30] K. Maca, H. Hadraba, J. Cihlar, Study of sintering of ceramics by means of high-temperature dilatometry, Ceramics-Silikáty 42 (1998) 151–158.
[31] M.J. Mayo, Processing of nanocrystalline ceramics from ultrafine particles, Int. Mater. Rev. 41 (1996) 85–115.
[32] K. Maca, H. Hadraba, J. Cihlar, Study of sintering of oxide ceramics at constant rate of heating and by means of rate-controlled sintering method, in: G. Mueller (Ed.), Ceramics-Processing, Reliability, Tribology and Wear, Wiley, VCH, 2000, pp. 161–166.
[33] A. Krell, A new look at grain size and load effects in the hardness of ceramics, Mater. Sci. Eng. A 245 (1998) 277–284.
[34] C. Zhao, J. Vleugels, L. Vandeperre, B. Basu, O. Van Der Biest, Y-TZP/Ce-TZP functionally graded composite, J. Mater. Sci. Lett. 17 (1998) 1453–1455.
[35] D.R. Bush, Designing ceramics components for structural applications, J. Mater. Eng. Perform. 2 (1993) 851–862.